Analytical and Bioanalytical Chemistry (2023) 415:3535–3547
https://doi.org/10.1007/s00216-023-04743-2

RESEARCH PAPER

Rapid detection of EGFR mutation in CTCs based on a double spiral microfluidic chip and the real-time RPA method

Wen-Man Li[1] · Xiao-Dong Ren[1] · Yu-Zhu Jiang[2] · Ning Su[1] · Bo-Wen Li[1] · Xian-Ge Sun[1] · Ruo-Xu Li[1] · Wei-Ping Lu[1] · Shao-Li Deng[1] · Jin Li[1] · Meng-Xia Li[2] · Qing Huang[1]

Received: 18 February 2023 / Revised: 8 May 2023 / Accepted: 10 May 2023 / Published online: 31 May 2023

Abstract

Circulating tumor cells (CTCs) are cells shed from primary or metastatic tumors and spread into the peripheral bloodstream. Mutation detection in CTCs can reveal vital genetic information about the tumors and can be used for "liquid biopsy" to indicate cancer treatment and targeted medication. However, current methods to measure the mutations in CTCs are based on PCR or DNA sequencing which are cumbersome and time-consuming and require sophisticated equipment. These largely limited their applications especially in areas with poor healthcare infrastructure. Here we report a simple, convenient, and rapid method for mutation detection in CTCs, including an example of a deletion at exon 19 (Del19) of the epidermal growth factor receptor (EGFR). CTCs in the peripheral blood of NSCLC patients were first sorted by a double spiral microfluidic chip with high sorting efficiency and purity. The sorted cells were then lysed by proteinase K, and the E19del mutation was detected via real-time recombinase polymerase amplification (RPA). Combining the advantages of microfluidic sorting and real-time RPA, an accurate mutation determination was realized within 2 h without professional operation or complex data interpretation. The method detected as few as 3 cells and 1% target variants under a strongly interfering background, thus, indicating its great potential in the non-invasive diagnosis of E19del mutation for NSCLC patients. The method can be further extended by redesigning the primers and probes to detect other deletion mutations, insertion mutations, and fusion genes. It is expected to be a universal molecular diagnostic tool for real-time assessment of relevant mutations and precise adjustments in the care of oncology patients.

Keywords Circulating tumor cell · Non-small cell lung cancer · Targeted medication · EGFR mutation detection · Microfluidic chip · Recombinase polymerase amplification

Introduction

Circulating tumor cells (CTCs) are tumor cells that leave the primary tumor and spread into the peripheral blood circulation [1]. They have been confirmed to be closely related to human cancer development, relapse, and metastasis [2–4]. CTCs contain detailed biological information about the primary tumor cells, and thus the mutation profiles in CTCs are powerful biomarkers for precision medicine of various human carcinomas, including non-small cell lung cancer (NSCLC).

NSCLC has high morbidity and mortality. It accounts for approximately 80–85% of human lung cancers [5]. Previous studies have shown that targeted treatments with EGFR-tyrosine kinase inhibitors (EGFR-TKIs) (e.g., gefitinib, erlotinib) were effective in most NSCLC patients. However, its efficacies are closely correlated with the EGFR gene mutation status at exons 18–21 in the tyrosine kinase coding domain [6–8]. The most prevalent EGFR kinase domain mutations are exon 19 mutations, characterized by in-frame deletions of amino acids 747–750, accounting for 45% of EGFR mutations in NSCLC. The L858R substitution in exon 21 comprises another 40–45% [9, 10]. Clinical trials have shown that NSCLC patients with exon 19 deletion (E19del) mutations responded better to gefitinib and erlotinib than

✉ Meng-Xia Li
mengxia.li@outlook.com

✉ Qing Huang
qinghuang@tmmu.edu.cn

[1] Department of Laboratory Medicine, Daping Hospital, Army Medical University, Chongqing, China

[2] Department of Cancer Center, Daping Hospital, Army Medical University, Chongqing, China

those with L858R point mutations [11]. In clinical practice, EGFR mutations are often analyzed in tumor tissue samples (e.g., tissue biopsy, or surgical operations) from NSCLC patients [12, 13]. However, these procedures have many disadvantages: they are painful to patients; it is difficult to obtain histopathological specimens depending on lesion location and pathological stage; and longitudinal tissue sampling is impossible. Therefore, this study was performed to analyze the EGFR mutations present in peripheral blood CTCs from NSCLC using E19del as an example. This approach can overcome the disadvantages described above.

The main strategies used to detect CTC mutations are PCR-based methods [14–16]—including amplification refractory mutation system (ARMS-PCR), real-time quantitative PCR (RT-qPCR), and droplet digital PCR (ddPCR)—as well as DNA sequencing [17, 18] (e.g., Sanger sequencing, pyrosequencing, next-generation sequencing). However, as valuable as these methods are, the cumbersome manual operation, time-consuming procedures (from hours to days), and the requirement for sophisticated equipment (e.g., DNA sequencer or thermocycler) have largely limited their applications [19, 20]. Because of the above-described reasons, it is especially problematic in areas with limited resources. Therefore, developing a more convenient and simple method to break the limitations and benefit more people is particularly important.

Recombinase polymerase amplification (RPA) is a well-performing isothermal nucleic acid amplification technology and a useful tool for nucleic acid amplification. Unlike PCR, RPA is based on the synergy of enzymes and proteins and does not require template denaturation [21]. The elimination of thermal cycling steps during gene amplification greatly shortens its reaction time (15–30 min) and helps it eliminate the need for temperature control [22, 23]. The RPA reaction can be performed under different conditions at a relatively low and constant temperature (37–42 ℃). It can even be initiated by the heat of human bodies [24, 25], which is particularly suitable for portable detection devices. Compared with other isothermal nucleic acid amplification technologies, RPA has advantages in sensitivity, specificity, detection speed, application range, and maneuverability [26–28]. For example, compared with the loop-mediated isothermal amplification (LAMP), another most commonly used isothermal nucleic acid amplification technology, the RPA method exhibits advantages with lower reaction temperature (60–65 ℃ for LAMP) and simpler primer design (2 primers for RPA and 4–6 primers for LAMP) [29]. Thus, the RPA technology has been rapidly developed in recent years and is widely applied to detect pathogens [30–34].

However, RPA has not yet been fully developed for human gene mutation detection. Only two related assays have been reported to date. The first combined the RPA method with an optical quantum sensor to detect point mutations in KRAS [35]. The overall construction of the assay is complex and time-consuming because the primer needs to be fixed on the sensor surface in advance, and the surface cleaning is very troublesome. Another assay used the RPA method to detect EGFR deletion mutations [36], but this is not a one-step detection method. The detection result was determined by staining amplified products with SYBR Green I dye. The method's selectivity was only 30–40%, which is insufficient in many clinical practices. Therefore, it is necessary to promote further RPA-related research to detect human gene mutations rapidly. Moreover, no report describes the RPA method for mutation detection in CTCs.

Here, a sensitive and rapid real-time RPA system was established and used to detect the E19del mutation in CTCs. Whole blood was first collected from NSCLC patients and diluted to an optimal hematocrit. The diluted blood was injected into a double spiral microfluidic chip at an optimized flow rate. After two-stage sorting, CTCs were collected from the target outlet while most of the other cells flowed out of the waste outlets. Two methods were used to detect the resulting CTCs: one was immunofluorescence staining for cell identification, and another one was cell lysis for mutation detection. The results showed that the double spiral microchip efficiently isolated the CTCs in the clinical blood samples. Furthermore, the CTC E19del mutations were successfully detected by the currently developed RPA system in all patients with EGFR mutational status known from tumor biopsies. Based on our knowledge, it is the first time an isothermal nucleic acid amplification technology was applied to mutation detection in CTCs. The current study offers a rapid, reliable, non-invasive mutation detection tool for cancer diagnosis, therapy, and prognosis.

Materials and methods

Preparation of samples

Cell line and culture

This work used the human non-small cell lung cancer cell line HCC-827 with a homozygous E19del mutation (i.e., E746-A750del) as the mutant-type (MT) cell sample. The HCC-827 cell was purchased from Procell Life Science & Technology Co., Ltd (Wuhan, China) and was maintained in RPMI-1640 medium (Gibco, USA) supplemented with 10% fetal bovine serum (HyClone, USA) and 1% penicillin–streptomycin (HyClone, USA) under standard growth conditions of 37 ℃ and 5% CO_2. Prior to the experiment, the HCC-827 cells were detached from the surface of the culture flask using 0.25% trypsin–EDTA (Gibco, USA) and centrifuged at 300 × *g* for 4 min and then resuspended in

phosphate-buffered saline (PBS; HyClone, USA) with 1% BSA (v/v; Sigma, USA).

Blood sample collection

This study was approved by the ethics committee of the Army Medical Center, and written informed consent was obtained from the patients or their family members before sample collection. All experiments were performed following relevant guidelines and regulations. The peripheral blood from healthy volunteers and carcinoma patients was collected in vacutainer tubes coated with EDTA-K2 anticoagulant. All carcinoma patients were diagnosed with NSCLC according to the International Association for the Study of Lung Cancer lung cancer staging protocol. The clinical descriptors of the participants are summarized in Supplementary Information (see Electronic Supplementary Material Table S1).

Lymphocyte separation from the peripheral blood of healthy volunteers

According to the manufacturer's introduction, the lymphocytes in the peripheral blood were isolated by using a lymphocyte separation medium (Solarbio, China). These cells were used as wild-type (WT) cell samples to evaluate the performance of the RPA system.

Genomic DNA extraction and quantification

The genomic DNA (gDNA) of the harvested HCC-827 cells was extracted using a QIAamp DNA Mini Kit (Qiagen, Germany) according to the manufacturer's instructions and used as MT-gDNA. The gDNA in the peripheral blood of healthy volunteers was extracted using QIAamp DNA Blood Mini Kit (Qiagen, Germany) and used as WT-gDNA. The gDNA concentrations were quantitatively determined using a Nanodrop 2000 UV–Vis spectrophotometer (Thermo Fisher Scientific, USA). The samples were stored at − 20 ℃ until use.

Quality control (QC) plasmid preparation and quantification

Here, E19del WT- and MT-gene fragments containing the target sequences were artificially synthesized by Sangon Biotech Co., Ltd (Shanghai, China) and cloned into a plasmid to prepare WT- and MT-QC plasmids. The sequences of all QC plasmids were confirmed by DNA Sanger sequencing (see Electronic Supplementary Material Fig. S1). The QC plasmids were then serially diluted, and the concentrations were quantified by digital PCR (ddPCR) (see Electronic Supplementary Material Fig. S2 and S3).

Cell lysis

Mutation detection directly after simple CTC lysis was needed to avoid the loss of CTCs during nucleic acid extraction and purification. Therefore, three different lysis methods were tested: ultrasound, proteinase K incubation, and direct PCR buffer. In the ultrasound method, a 100 µl cell suspension was added into an Eppendorf tube and treated with an ultrasonicator (Diagenode Bioruptor; Belgium; five 30-s on/off cycles). In the proteinase K incubation method, proteinase K (Qiagen, Germany) and cell suspensions were mixed at a ratio of 1:10, incubated in a bath (TIANGEN, China) at 56 ℃ for 10 min, and then inactivated at 95 ℃ for 10 min. In the direct PCR buffer method, 10 µl of the direct PCR buffer (Koma BioTech, Korea) was added directly to the RPA reaction system [31]. The cell lysates obtained by the three lysis methods were then detected by the real-time RPA method developed here. The lysis efficiency was evaluated according to the amplification curves.

Design and evaluation of the real-time RPA system

Design of the real-time RPA reaction system

A pair of RPA primers to amplify the mutant and wild-type gene sequences simultaneously were designed based on the deletion-mutation site of EGFR exon 19. Fluorescence detection used fluorophore/quencher probes specific for wild-type and mutations. The primers and probes were synthesized by Sangon Biotech (Shanghai, China) and Beijing Genomics Institute (Shenzhen, China), respectively. The sequences for the RPA primers and probes are listed in Table 1.

An Exo kit (Amplification Future, China) consisting of freeze-dried reagent (a mixture of recombinase, polymerase, exonuclease, and single-strand binding protein), a rehydration buffer, and $Mg(OAc)_2$ solution was used for the real-time detection of the E19del mutation. A mixture containing rehydration buffer, forward primer (400 nM), reverse primer (400 nM), WT probe (80 nM), MT probe (120 nM), optimized templates, and water was added to the freeze-dried reagent pellet. The $Mg(OAc)_2$ solution was then added. Finally, the RPA reaction was performed at 39 ℃ for 20 min on a Bio-Rad CFX connected real-time PCR detection system (Bio-rad, USA).

Performance evaluation of the real-time RPA method

Sensitivity and selectivity are two of the most important property parameters of a mutant detection system [37–39]. The sensitivity indicates the lowest amount of the target mutant that an assay can detect (also known as the limit of detection). The selectivity refers to the capacity to detect

Table 1 Oligonucleotides for the RPA reaction system

Target	Oligo ID	Description	Oligo sequence (5' > 3')
EGFR	DP-4	R. Ef-primer[a]	GGCACCATCTCACAATTGCCAGTTAACGTCTTCC
	DP-6	R. Er-primer[b]	GACATGAGAAAAGGTGGGCCTGAGGTTCAGAG
	DP-9	R.E-probe-MT[c]	CATCGAGGATTTCCTTGTTGGCTTTCGGAG ATG[FAM-dT][THF][BHQ1-dT]TGATAGCGACGG GAAT (C3-spacer[d])
	DP-15	R.E-probe-WT[e]	CACATCGAGGATTTCCTTGTTGGCTTTCGG AGA[VIC-dT][THF][BHQ1-dT]TGCTTCTCTTAA TTCCTTG (C3-spacer)

[a]Forward primer targeting EGFR gene for RPA, [b]reverse primer targeting EGFR gene for RPA, [c]mutant-type probe targeting EGFR gene for RPA, [d]spacer modifications at the 3′-terminal base, [e]wild-type probe targeting EGFR gene for RPA

MT genes among an excess of WT genes and was defined as the ratio of copy number between the MT gene and the total gene including both WT and MT genes. The sensitivity of the real-time RPA method was determined by serially diluted MT-QC plasmids (5, 10, 100, 1000, 10,000 copies), MT-gDNA (4 pg, 8 pg, 16 pg, 32 pg, 320 pg, 3.2 ng, 32 ng, and 320 ng) and MT-cell (2.5, 25, 250, 2500 cells/reaction). Furthermore, the selectivity of the real-time RPA method was determined by spiking the three different MT samples to their corresponding WT samples at different percentages (e.g., 90%, 50%, 10%, and 1%).

Structure and principle of the double spiral microchip

A double spiral microfluidic chip constructed by our team [40] was used to isolate the CTCs of NSCLC patients. The chip employs two internally connected single spiral microchannels with inverse directions (Fig. 1). The forward flow is described as the 1st spiral microchannel (pink arrow and pink channel in Fig. 1a), and the backward flow is called the 2nd spiral microchannel (blue arrow and blue channel in Fig. 1a). The two spiral microchannels are connected to three inlets—namely the sample inlet, the 1st sheath inlet, and the 2nd sheath inlet (marked i, ii, iii in Fig. 1a, respectively). There are also three outlets: the 1st waste outlet, the 2nd waste outlet, and the target outlet (marked iv, v, vi in Fig. 1a, respectively). All inlets and outlets are extended to the periphery of the microchip to facilitate the connection with outer tubing and to ensure a better viewing field.

During the sorting process, the sample and the 1st sheath fluid flow into the 1st spiral microchannel in a laminar flow state. The 2nd sheath fluid was pumped into the 2nd spiral microchannel alone. The double spiral microfluidic chip is

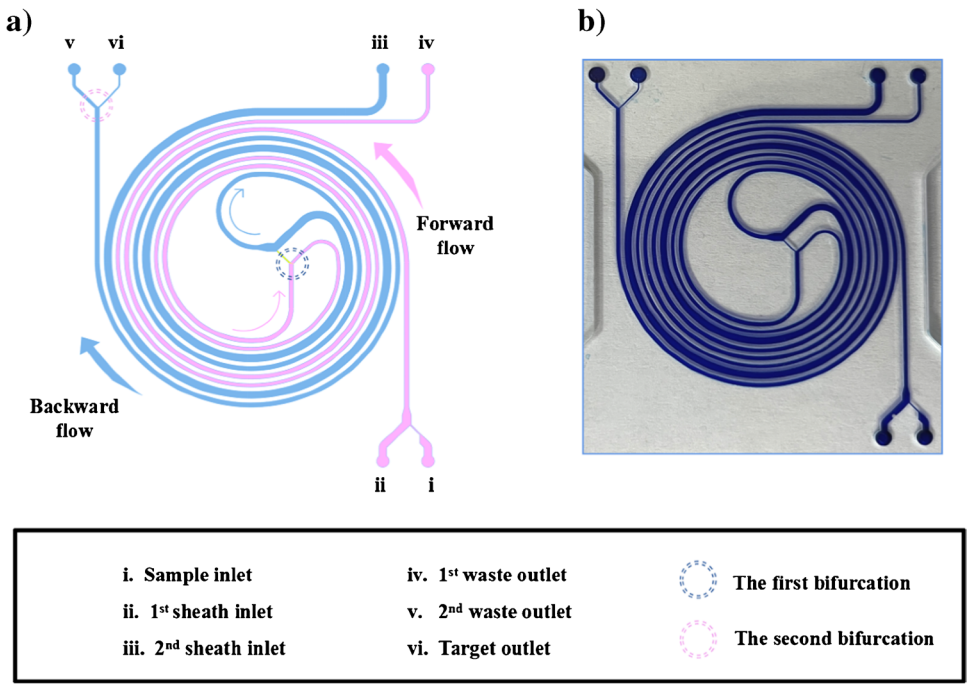

Fig. 1 Structure of the double spiral microfluidic chip for CTCs isolation. **a** Schematic diagram of the double spiral microfluidic chip. The 1st spiral microchannel and 2nd spiral channel are marked in pink and blue, respectively. The inlets and outlets are marked with serial numbers i, ii, iii and iv, v, vi respectively. The pink arrows and blue arrows represent the forward flow in the first and the backflow in the second microchannel, respectively. The blue and pink dashed circles indicate the first and the second bifurcation, respectively. **b** Photograph of the double spiral microfluidic chip. The microchannels were filled with blue ink for better observation

a label-free hydrodynamic size separation method, which is based on the initial focusing. Cells in the spiral microchannel will obtain a size-dependent equilibrium position according to the balance of multiple forces [41]. In the 1st spiral microchannel, cells with different sizes are positioned at different positions under the interaction of inertial lift force and Dean drag force [42]. CTCs (much larger) are focused close to the inner wall of the channel and flow into the 2nd spiral microchannel at the first bifurcation (blue dashed circle in Fig. 1a). Small cells (i.e., RBCs and WBCs) migrated to the outer wall along with the Dean vortices and eventually flowed to the 1st waste outlet. Most RBCs and WBCs were removed after the first stage of spiral inertial sorting, but there were still some blood cells of similar size as CTCs entering into the second microchannel. In the 2nd spiral microchannel, a curved and focused sample flow segment was formed using a simple channel geometry with the help of asymmetry sheath flow. The results produced a soft inertial deflection effect on the particles. The soft inertial particle deflection is a simple and size-based method that is especially advantageous for separating cells or particles of similar size under which the large and small cells are deflected to different degrees in streamlines and then eventually separated [43] at the second bifurcation (pink dashed circle in Fig. 1a). In this way, residual smaller blood cells were again removed for secondary purification of CTCs. Finally, the targeted CTCs were collected from the inner wall of the 2nd spiral microchannel via the target outlet while other cells flowed out of the 2nd waste outlet.

Characterization of the double spiral microchip

Preparation of the sample

Firstly, fluorescence staining was performed on the HCC-827 cells to distinguish tumor cells from the blood cells. HCC-827 cells were suspended in Cell Tracker Green CMFDA Dye (Invitrogen, USA) at 10^6 cells/ml and incubated at 37 ℃ and 5% CO_2 for 30 min. After incubation, cells were centrifuged at 300 × g for 5 min. The supernatant was discarded, and the cells were washed with PBS at least three times. Then, the CMFDA-labeled HCC-827 cells (10^2–10^3 cells/ml) were spiked into the peripheral blood of healthy volunteers to simulate clinical NSCLC samples. All processes were protected from light.

Experimental setup

The double spiral microchip was mounted on the carrier stage of an inverted microscope (Olympus IX73, Japan). Videos and images during the sorting process were continuously acquired with a high-speed camera (FASTCAM NOVA S9, USA). The flow rate was controlled by a double-channel precision syringe pump (Longer Pump, China). During the injection, a magnetic stirrer (V&P Scientific Inc., USA) was used to ensure the sample's uniform distribution of cells. The concentrations of the samples were determined using a blood cell counting plate.

Performance evaluation of the microchip

The simulated sample and the 1st and 2nd sheaths were pumped into the double spiral microfluidic chip at a flow rate of 300 µl/min, 650 µl/min, and 500 µl/min, respectively. The separation efficiency and purity were calculated by counting the number of HCC-827 cells and non-tumor cells from the target outlet. Then, the flow rate of the 2nd sheath was adjusted from 500 to 650 µl/min to investigate the separation efficiency and purity under different experimental conditions.

Detection of clinical samples

Isolation of CTCs from the peripheral blood of NSCLC patients

The peripheral blood of the patients was diluted to a hematocrit of 4% according to our previous research and then injected into the first-stage inlet of the double spiral chip at 300 µl/min. The 1st and 2nd sheath flows were injected into the double spiral chip at 650 µl/min and 550 µl/min, respectively. After cell sorting, CTCs were collected in sample tubes connecting the target outlet, and the waste solution was discharged from the waste outlet. Isolated cells were collected from the outlet (~ 20 ml volume) and divided into two parts. One part was taken for immunostaining, and the other was for mutation detection.

Immunofluorescence staining of the sorted cells

Immunofluorescence of sorted cells from 10 NSCLC patients was first performed at random to verify the presence of the isolated CTCs. To avoid cell loss, the immunofluorescence staining was performed on a 4 µm membrane filter (Merck Millipore Ltd, Ireland). The cell suspensions were first dropped on the filter membrane to fix the cells and repeated three times. The CTCs were then immunostained with FITC-cytokeratin antibody (CK; Miltenyi Biotec, Germany) and washed three times with PBS. Cells were then incubated with PE-CD45 antibody (Miltenyi Biotec, Germany) to identify the white blood cells (WBC). Finally, cell nuclei were stained with 4',6-diamidino-2-phenylindole (DAPI; Beyotime, China) for 5–15 min. After immunofluorescence staining, cells were washed with PBS for image acquisition and cell counting via a fluorescence microscope.

Mutation detection of CTCs by RPA and validation with clinical diagnostics

After sorting via the double spiral microfluidic chip, the cells were centrifuged at 600 × g for 15 min. The supernatant was then discarded, and the cells were lysed. Cell lysates were then added to the RPA reaction mixture as crude templates, and the E19del mutation was detected via the constructed RPA system. The E19del mutation status of all NSCLC patients had already been determined via biopsy tissues using a commercially available ARMS-PCR kit (AmoyDx, China). The ARMS-PCR was performed following the manufacturer's instructions and standard clinical procedures. Both the RPA and ARMS-PCR reactions were performed on a CFX96 Real-Time PCR platform (Bio-Rad, USA). The results of the two methods were compared and analyzed.

Results and discussion

With the popularity of precision medicine, developing reliable biomarkers to guide the selection of the most appropriate therapies for individual patients has become increasingly important. Compared to conventional tissue biopsies, circulating biomarkers in the peripheral blood, such as circulating tumor cells (CTCs), have enormous potential as repeatable, non-invasive, cost-effective "liquid biopsies." It has been confirmed that CTCs are closely related to human cancer development, relapse, and metastasis [44, 45]. The main clinical applications of CTCs focused on the enumeration of CTCs, which have prognostic value in a wide range of malignancies [46]. However, increasing evidence shows that moving beyond the enumeration towards more sophisticated molecular analyses may be useful for better patient stratification [47, 48]. Genetic mutation is one of the most common molecular alterations in tumors that may represent drug-targeting opportunities. EGFR-mutated NSCLC is a good illustration [49]. The EGFR-mutated NSCLC is a genetically heterogeneous disease with more than 200 distinct mutations. The most common deletion mutation at exon 19, codons 746–750, predicts sensitivity to EGFR tyrosine kinase inhibitors (TKIs) [11, 49]. Detection of the mutation in CTCs may serve as predictive biomarkers to guide the use of targeted therapies with selective activity against tumors harboring these alterations [48]. The main strategies used to detect CTC mutations are PCR-based methods and DNA sequencing. However, the cumbersome manual operation and the requirement of sophisticated apparatus seriously hinder their application in areas with poor healthcare infrastructure. Thus, in this paper, we developed a simple, rapid, and specific real-time RPA method to detect the E19del mutation in CTCs.

Principle of the E19del mutation detection by real-time RPA

The wild-type and E19del mutant sequences were amplified simultaneously via a pair of universal primers in the real-time RPA system. Two specific Exo probes were designed to determine the genotypes of the amplicon. Both probes consist of an oligonucleotide with homology to the target amplicon, a fluorophore, a quencher (e.g., Black Hole Quencher, BHQ) to temporarily deter the fluorescent signal, and a blocker at the 3'-end (Fig. 2a). They differed in their oligonucleotide sequences and labeled fluorophores. The WT probe contained a complete wild-type sequence at exon 19 that can only specifically bind to wild-type samples. The sequence of the MT probe crossed the E746-A750 fragment and can only specifically bind to the mutant sequence with in-frame deletions of E746-A750. The probe can be cleaved at the abasic site (e.g., tetrahydrofuran, THF) to produce fluorescence only after binding with the target sequence (Fig. 2b). Probe cleavage is thus indicative of a specific target amplification event and can be used to monitor specific amplicon accumulation.

Performance evaluation of the real-time RPA method

The sensitivity and selectivity of the system were evaluated via QC plasmids as a standard sequence control first. The results showed that the E19del mutation could be accurately determined with sequence specificity within 20 min via a simple step, which is significantly faster and more convenient than the traditional PCR and DNA sequencing. The detection sensitivity and selectivity of the system were shown to be 10 copies and 10%, respectively (Fig. 3a and d).

Then, genomic DNA extracted from cell samples was studied to further evaluate the system's reliability. It was shown that the RPA system was exquisitely sensitive and could detect as few as 4 pg of MT-gDNA (Fig. 3b), which is equivalent to a single copy. Similarly, by spiking MT-gDNA into excessive WT-gDNA, the system's selectivity in detecting gDNA samples was determined to be 1% (Fig. 3e), which can reach the level of PCR kits used in the clinic.

As traditional nucleic acid extraction and purification methods suffer cumbersome manual operation, CTC loss is inevitable. Direct analysis of cell lysates thus is much preferable. In this paper, three lysis methods were tested as described above. The results showed that cells lysed with proteinase K had the best amplification curve, a more standard sigmoidal characteristic, and the highest fluorescence intensity (see Electronic Supplementary Material Fig. S4). These indicated its superior lysis efficiency. Therefore, proteinase K was selected as the final cell lysis method. The HCC-827 cells were then serially diluted, lysed by proteinase K, and directly detected by

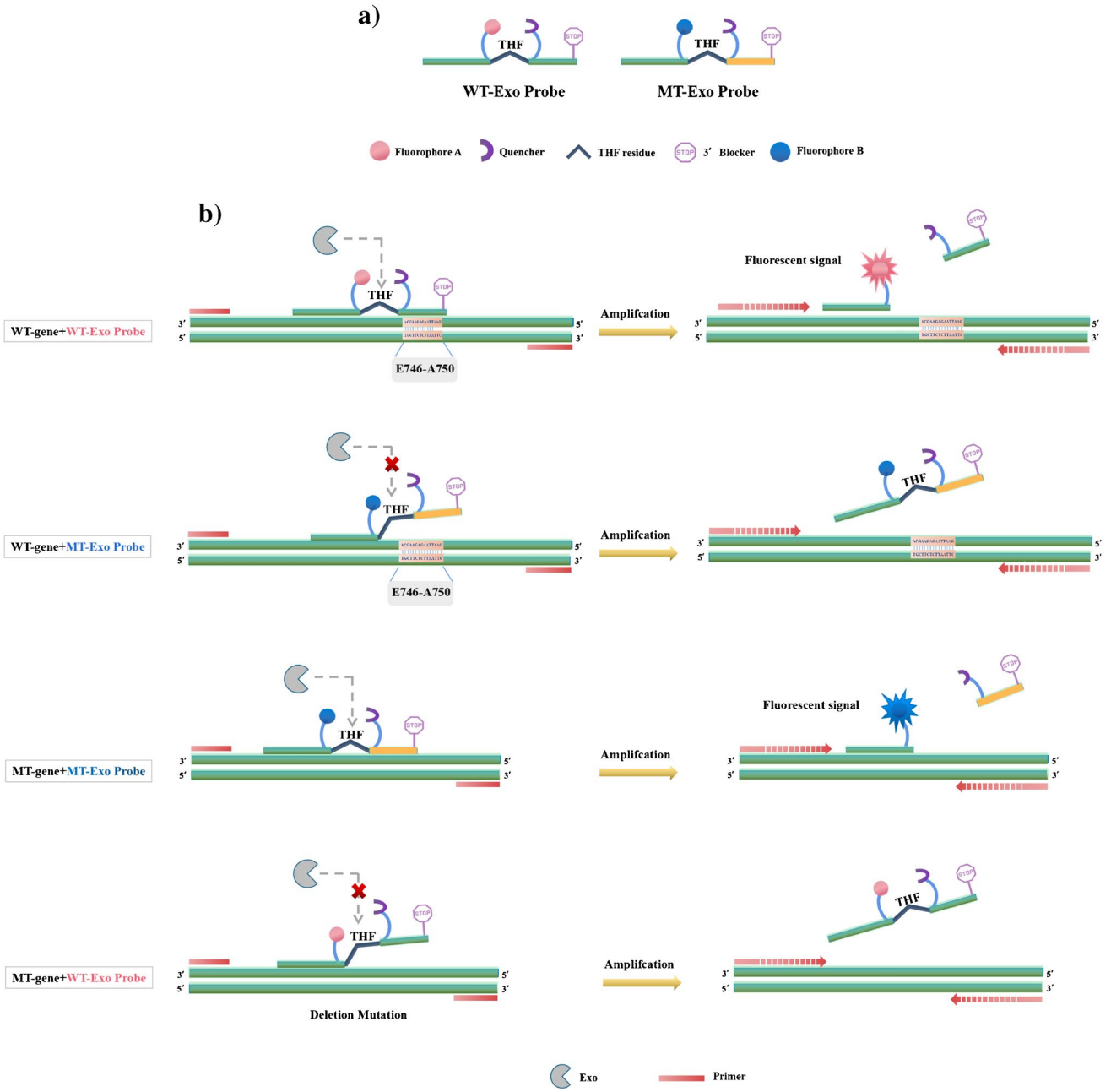

Fig. 2 Schematic of the E19del mutation detected by real-time RPA. **a** Construction of the probes. **b** Binding of the probes with different sequences and generating fluorescent signals. During strand extension, only the specifically bound probe can be cleaved by the *E. coli* exonuclease III at the THF to release the fluorophore from the quencher and generate a fluorescent signal

real-time RPA. The system was exquisitely robust to overcome the inhibition of cellular contents and the limit of the detection was 3 cells per 50 ml reaction, which has reached a single-cell detection level (Fig. 3c). HCC-827 cells were spiked into lymphocytes at different percentages to simulate sorted CTCs of different purities. The cell lysate mixture was directly detected after being lysed by proteinase K. The RPA method can identify the 1% of MT-cells in the WT-cells (Fig. 3f). The RPA system was sufficiently sensitive and robust to detect the E19del mutation in cell lysates, thus making it possible to directly detect the E19del mutation in CTCs via a simple isothermal nucleic acid amplification method.

Performance characterization of the double spiral chip

CTCs in the peripheral blood are extremely rare that might be as low as 1 CTC per ml of whole blood with billions

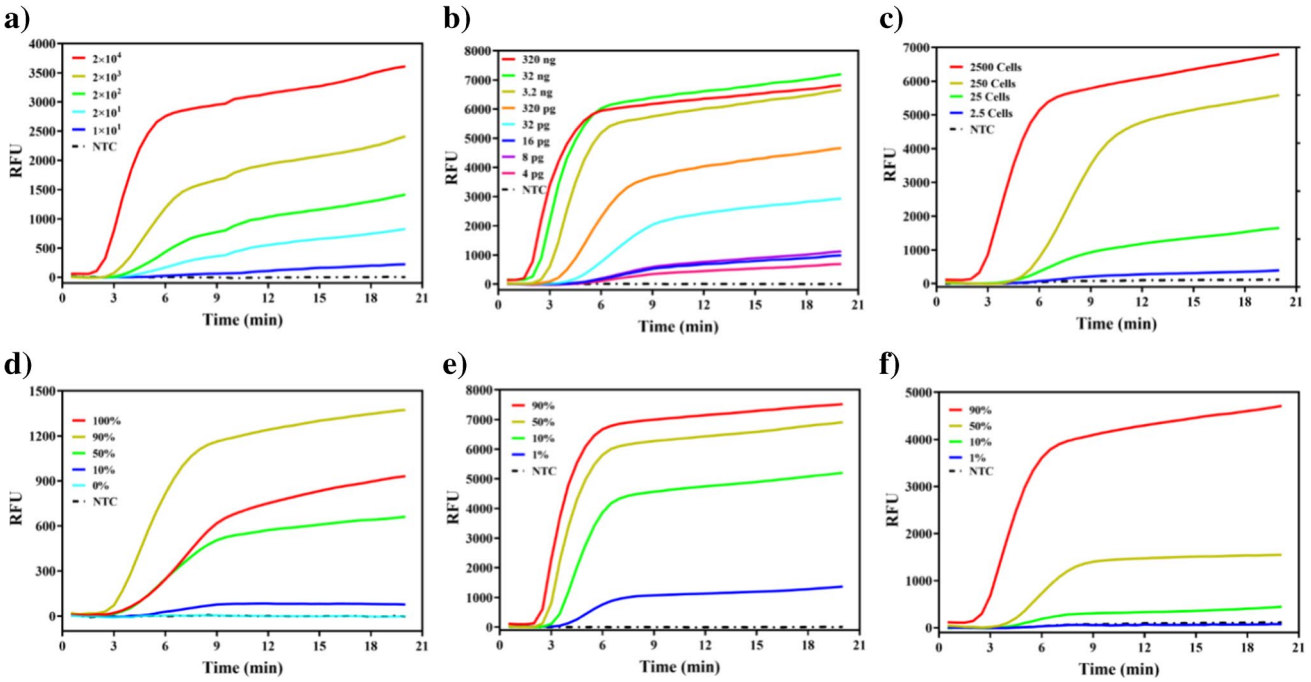

Fig. 3 Sensitivity and selectivity of the real-time RPA system. **a** Amplification curves of MT-QC plasmid at various amounts (i.e., 10, 20, 200, 2000, 20,000 copies). **b** Amplification curves of EGFR MT gene at various amounts (i.e., 4 pg, 8 pg, 16 pg, 32 pg, 320 pg, 3.2 ng, 32 ng, and 320 ng) of cell line HCC-827 gDNA. **c** Amplification curves of EGFR MT gene in MT-cells at different amounts (i.e., 2500, 250, 25, 2.5). **d** Detection of MT-QC plasmid spiked in the WT-QC plasmid at different percentages (i.e., 100%, 90%, 50%, 10%, and 0%). **e** Detection of MT-gDNA spiked in the WT-gDNA at different percentages (i.e., 90%, 50%, 10%, and 1%). **f** Detection of MT-cells spiked in the WT-cells at different percentages (i.e., 90%, 50%, 10%, and 1%)

of red blood cells (RBCs), millions of white blood cells (WBCs), and other background components. Efficient isolation of CTCs is necessary and crucial. Currently, there are many different methods for CTC isolation, which can be roughly divided into two categories based on their principles. One is the immune capture based on cell surface markers and another is the physical sorting relying on differences in the cell's physical properties [50]. However, due to the heterogeneity of tumors, the molecular expression and phenotype of CTCs showed great differentiation [51–53]. Immune capture still has major limitations in the efficient sorting of CTCs, and thus in this study a double spiral microfluidic chip based on the cell's physical property (size differences) was used. Unlike the other physical sorting methods such as centrifugation [54], dielectrophoresis [55], magnetic method [56], and acoustic capture [57], the double spiral microfluidic chip utilizes inertial focusing to create size-dependent separation of the cells. Hence, it does not require additional physical fields, specific geometries, and controlled microfabrication, which greatly simplifies the structure and fabrication of the devices [58], and a higher throughput and a more robust implementation can also be obtained. While comparing with other existing techniques for inertial sorting of CTCs (e.g., single spiral microfluidic chips), the double spiral microfluidic chip combined the effects of two-stage inertial focusing and particle deflection. The 1st spiral microchannel can remove most RBCs and WBCs with obvious size differences with CTCs by the interaction of inertial lift force and Dean drag force [42]. The 2nd spiral microchannel was designed to produce a soft inertial deflection effect on the cells to remove the residual smaller blood cells of similar size as CTCs. As a result, a secondary purification of CTCs will be obtained. Simple sample pretreatment, low sample loss, and high separation efficiency are unique advantages of the double spiral microfluidic chip.

Separation efficiency (also called the recovery rate) and separation purity are the two most important parameters to evaluate sorting performance. According to our previous research [40], the flow rate of the 2nd sheath has the most significant effect on cell deflection and separation. Therefore, the flow rate of the 2nd sheath was adjusted from 500 to 650 µl/min. Figure 4a shows that the focus and deflection efficiency of the 1st stage spiral microchannel is improved with increasing the 2nd sheath flow rate. This result implies that fewer blood cells entered the second-stage microchannel, thus resulting in a relatively high sorting purity. It also indicates a loss of some smaller tumor cells as they were deflected into the 1st waste channel with similar blood cells, thus reducing sorting efficiency. By immunofluorescence staining, no CTC was observed in the 2nd waste, confirming

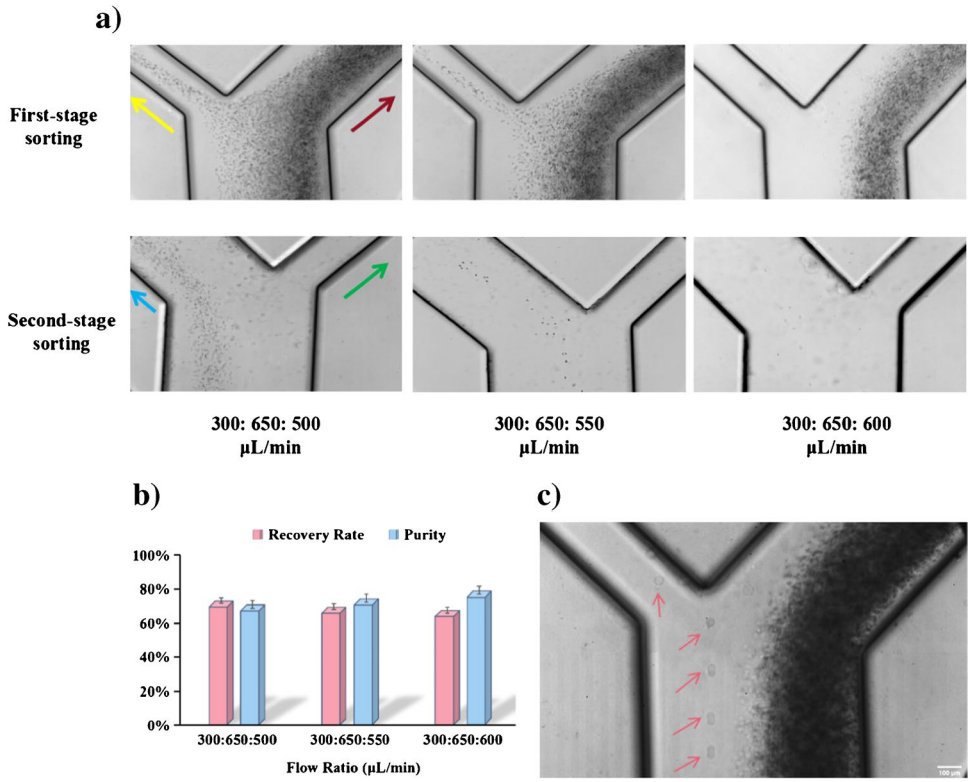

Fig. 4 Performance characterization of the double spiral chip. **a** Deflection of the cells under different flow rates of the 2nd sheath (500, 550, and 600 µl/min, respectively). The yellow arrow indicates the cells that deflect into the 2nd spiral microchannel while the red arrow indicates the cells that deflect to the 1st waste outlet. The blue arrow indicates the cells that deflect to the 2nd waste outlet while the green arrow indicates the cells flow to the target outlet. **b** Recovery rates and separation purity of HCC-827 cells from mimic clinical samples at different flow rates of the 2nd sheath. **c** Movement trajectories of a tumor cell (HCC-827) (indicated by the red arrows) in the 1st spiral microchannel (Stacks processing by Adobe Photoshop 2021). Scale bar, 100 µm

that the loss of CTCs mainly occurred in the first stage separation. Statistical results of three experiments are shown in Fig. 4b. When the flow rate of the 2nd sheath was 550 µl/min, the separation efficiency and purity can both be more than 70%. Thus, considering a balance of the two parameters, a flow rate of 550 µl/min was selected in this study to process clinical blood samples. Moreover, Fig. 4c shows the movement trajectories of a tumor cell (HCC-827) (indicated by the red arrows) in the 1st spiral microchannel under the selected flow rate.

Detection of clinical samples

Peripheral blood samples from human subjects with NSCLC were tested next to validate the clinical utility of the workflow for identifying the E19del mutation. Here, 4 ml of blood was collected from 20 NSCLC patients including 10 positives and 10 negatives for the E19del mutation. Each blood sample was sorted via the double spiral microfluidic chip at a flow rate set of 300:650:550 µl/min. The trajectories of CTCs during the separation were captured by high-speed CCD (see Electronic Supplementary Material Video S1). After two-stage sorting, most blood cells were discarded from the 1st and 2nd waste outlets, and the sorted CTCs were collected from the target outlet.

In order to verify the presence of the isolated CTCs, immunofluorescence staining was performed on 10 samples at random. The DAPI + -CD45 − -CK + cells were regarded as CTCs, and DAPI + -CD45 + -CK - cells were considered WBCs (Fig. 5a). The CTCs were detected in all 10 patients with counts ranging from 5 to 35 CTCs per 2 ml of blood (Fig. 5b). This verified the high sensitivity of the double spiral microchannel for isolating CTCs. The number of CTCs should be slightly higher than the counted number due to tumor cells' high phenotypic expression heterogeneity and cell loss during centrifugation. Moreover, there were several rounds of washing during immunostaining [59]. In addition, it should be noted that no bright field image was captured as the immunofluorescence staining of the sorted cells was performed on a black, opaque membrane filter. However, the identification results of CTCs would not be affected.

Then, E19del mutation detection was carried out for the collected CTCs using the RPA method. CTCs were directly detected using real-time RPA after being lysed by proteinase K. The results showed that E19del mutation was detected in all 10 positive samples (Fig. 6), but no mutation was detected in any of the 10 negative samples (Fig. 7). It can be seen that positive samples showed obvious amplification curves and fluorescence intensity, while the negative samples did not. The results are completely consistent with the ARMS-PCR detection results in our hospital. Moreover, the conventional ARMS-PCR method takes several hours or even several days from sampling to producing results, while by combining the double spiral microfluidic chip and real-time RPA system, an accurate mutation determination without invasive sampling can be obtained only within

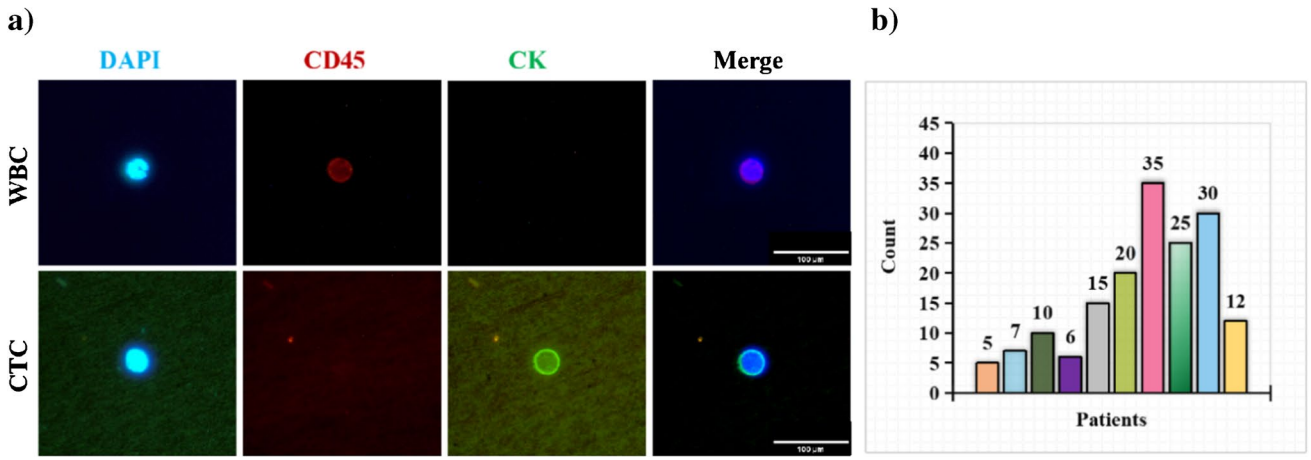

Fig. 5 Immunofluorescence staining of isolated cells. **a** Immunofluorescence staining of sorted cells. DAPI + -CD45 + -CK − cells were identified as WBC while DAPI + -CD45 − -CK + cells were scored as CTCs. Scale bar, 100 μm. **b** Count of isolated CTCs in 10 patients

2 h. It not only overcomes the intrinsic limitations of tissue biopsies but also breaks through the traditional laboratory boundaries by providing nucleic acid replication at constant temperatures. Compared with the traditional PCR method, the detection setup in this study exhibits advantages with low instrument requirements, simple operation, short reaction time, and robust resistance to inhibitors. In addition, lots of research have reported that microfluidic technology has unique advantages in single-cell gene mutation detection because of its high integration, portable size, and low consumption of reagents [60–62]. However, the high denaturation temperature of the PCR method (about 95 ℃) has largely limited its application in microfluidic platforms as it is very easy to cause chip deformation and reagent evaporation. Therefore, the real-time RPA method constructed in this paper is quite suitable for integrating microfluidic chips, as the temperature required is relatively mild (about 40 ℃), providing a promising simple, rapid, accurate, and sensitive mutation detection method in a single cell.

Of course, the currently described method still has some limitations. For example, only known specific mutations can be detected while unknown mutations would be overlooked. Moreover, in the current setup, only the E19del mutation was detected while there are multiple clinically relevant variations in the EGFR gene. The applicability of the real-time RPA method in detecting all the mutations needs to be further validated because of the inherent defect of the RPA method in detecting single-base mutations. Regarding this, we have conducted in-depth research and are striving to solve it by combining the build real-time RPA method with other novel approaches such as chemical and physical sensors. We will continue to improve our method to cover a wider range of variation types. In addition, unlike classical real-time PCR (or quantitative PCR), the real-time RPA method is not yet suitable for nucleic acid quantification as it is chemically initiated by adding magnesium acetate rather than being thermally initiated by increasing the reaction temperature to 95 ℃. Hence, the RPA reaction is based

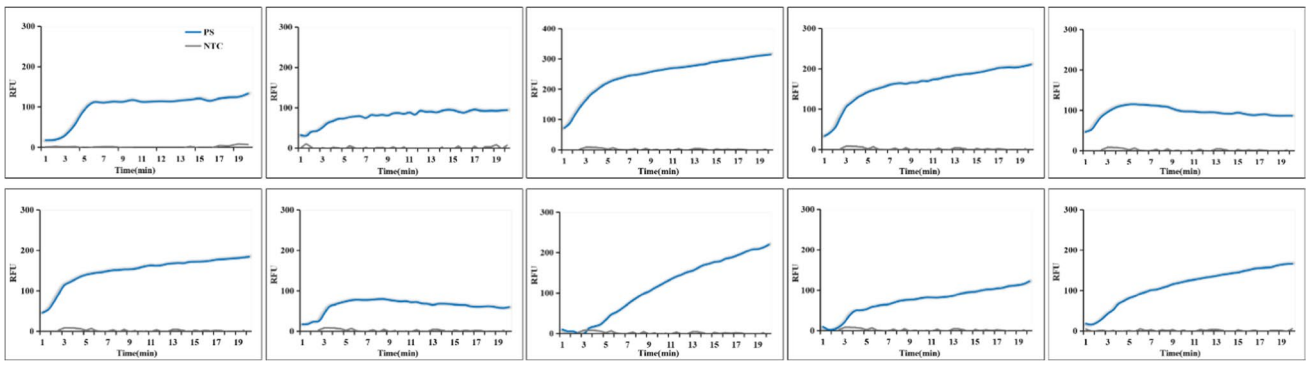

Fig. 6 Detection results of 10 positive clinical samples. The real-time RPA amplification curves of 10 NSCLC patients diagnosed with E19del mutation in our hospital

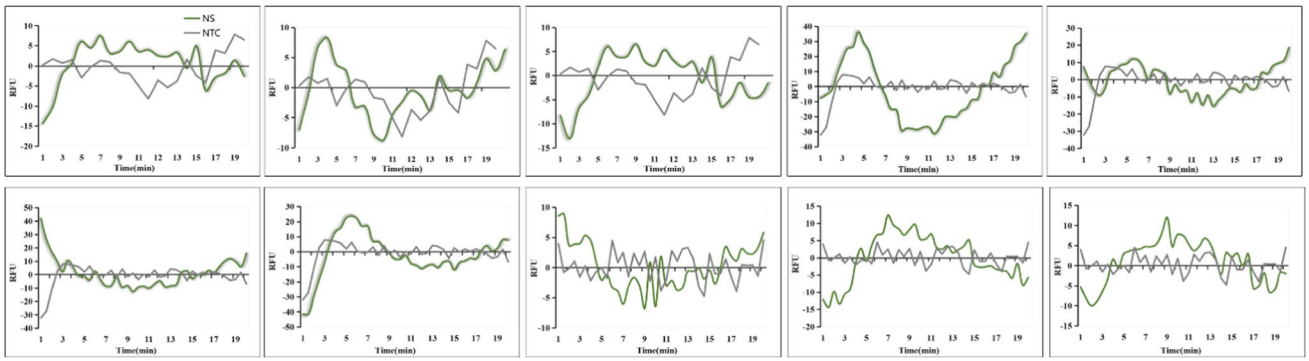

Fig. 7 Detection results of 10 negative clinical samples. The real-time RPA amplification curves of 10 NSCLC patients diagnosed without E19del mutation in our hospital

on a time threshold instead of a cycle threshold and this time threshold is dictated not only by the initial target concentration but also by the temperature and mixing step [63]. Thus, the reaction starting point cannot be precisely controlled. Meanwhile, the annealing occurs constantly at the optimal temperature for RPA reaction. This can produce a nonlinear calibration curve [22]. Slowing down the RPA reaction rate by decreasing the magnesium acetate concentration to have better control during the real-time RPA reaction may be a proper try. Furthermore, if the mutation detection results of the real-time RPA method can be confirmed by an absolute quantitative method (e.g., digital PCR), it would be much more convincing. However, due to the limited blood volume, this part of the content was not carried out and would be considered in subsequent studies. Moreover, other tumor types besides NSCLC could be involved and the clinical sample size might be further expanded.

Conclusions

In conclusion, a simple, rapid, and specific real-time RPA method was established in the current study. By combining with the advantages of microfluidic technology, the E19del mutation in CTCs was detected by the RPA method for the first time. An accurate determination of sequence specificity was obtained within 20 min, which is significantly faster and more convenient than the traditional PCR and DNA sequencing methods. The real-time RPA assay does not need thermal control equipment and has unique advantages for portable mutation detection. Furthermore, unlike most other methods, crude cell lysates without purification could be used directly here. The real-time RPA method could detect down to three cells and identify 1% deletion mutant variants in the context of strong interference. By redesigning the primers and probes, the method can be further extended to detect other deletion mutations, insertion mutations, and fusion genes. The method constructed here provides a new strategy for mutation detection in CTCs and may be adopted into rapid molecular diagnosis for people in areas with poor healthcare infrastructure.

Supplementary Information The online version contains supplementary material available at https://doi.org/10.1007/s00216-023-04743-2.

Author contribution Wenman Li and Qing Huang designed the research. Wenman Li and Xiaodong Ren performed the experiments. Yuzhu Jiang and Mengxia Li identified the donors and obtained the blood samples. Bowen Li, Xiange Sun, Ruoxu Li, and Jin Li organized the data. Wenman Li, Xiaodong Ren, and Ning Su analyzed the results and visualized the data. Wenman Li wrote the manuscript with assistance from all authors. Weiping Lu, Dengshao Li, and Qing Huang revised the paper. All authors have read and approved this manuscript.

Funding This study was supported by the National Natural Science Foundation of China (Grant No.: 82172370), Natural Science Foundation of Chongqing (Grant No.: cstc2020jcyj-msxmX0173), and Military Logistics Research Project (Grant No.: 2019XLC1010).

Declarations

Ethics approval The studies involving human participants were reviewed and approved by the Ethics Committee of Army Medical Center (Chongqing, China; Approved No. 2020P27). The patients/participants provided their written informed consent to participate in this study.

Conflict of interest The authors declare no competing interests.

Source of biological material The peripheral blood used in this study is from healthy volunteers and carcinoma patients at DaPing Hospital in Chongqing, China.

References

1. Gupta GP, Massague J. Cancer metastasis: building a framework. Cell. 2006;127(4):679–95.
2. Esmaeilsabzali H, Beischlag TV, Cox ME, Parameswaran AM, Park EJ. Detection and isolation of circulating tumor cells: principles and methods. Biotechnol Adv. 2013;31(7):1063–84.

3. Chaffer CL, Weinberg RA. A perspective on cancer cell metastasis. Science. 2011;331(6024):1559–64.
4. Hong B, Zu Y. Detecting circulating tumor cells: current challenges and new trends. Theranostics. 2013;3(6):377–94.
5. Crino L, Weder W, van Meerbeeck J, Felip E, Group EGW. Early stage and locally advanced (non-metastatic) non-small-cell lung cancer: ESMO Clinical Practice Guidelines for diagnosis, treatment and follow-up. Ann Oncol. 2010;21 Suppl 5:v103-15.
6. Pao W, Miller V, Zakowski M, Doherty J, Politi K, Sarkaria I, et al. EGF receptor gene mutations are common in lung cancers from "never smokers" and are associated with sensitivity of tumors to gefitinib and erlotinib. Proc Natl Acad Sci U S A. 2004;101(36):13306–11.
7. D'Incecco A, Cannita K, Martella F, De Vico A, Zaccagna G, Landi L, et al. Multidisciplinary and real life data: practical management of epidermal growth factor receptor (EGFR) mutant non-small cell lung cancer (NSCLC). J Thorac Dis. 2022;14(4):805–8.
8. Mitsudomi T, Yatabe Y. Epidermal growth factor receptor in relation to tumor development: EGFR gene and cancer. FEBS J. 2010;277(2):301–8.
9. Jackman DM, Yeap BY, Sequist LV, Lindeman N, Holmes AJ, Joshi VA, et al. Exon 19 deletion mutations of epidermal growth factor receptor are associated with prolonged survival in non-small cell lung cancer patients treated with gefitinib or erlotinib. Clin Cancer Res. 2006;12(13):3908–14.
10. Mitsudomi T, Kosaka T, Endoh H, Horio Y, Hida T, Mori S, et al. Mutations of the epidermal growth factor receptor gene predict prolonged survival after gefitinib treatment in patients with non-small-cell lung cancer with postoperative recurrence. J Clin Oncol. 2005;23(11):2513–20.
11. Riely GJ, Pao W, Pham D, Li AR, Rizvi N, Venkatraman ES, et al. Clinical course of patients with non-small cell lung cancer and epidermal growth factor receptor exon 19 and exon 21 mutations treated with gefitinib or erlotinib. Clin Cancer Res. 2006;12(3 Pt 1):839–44.
12. Liu X, Zhang C, Zhang S, Cai Y, Hua K, Cui Y. One-step determination of deletion mutation based on loop-mediated isothermal amplification. Anal Biochem. 2021;616:114087.
13. Marrugo-Ramirez J, Mir M, Samitier J. Blood-based cancer biomarkers in liquid biopsy: a promising non-invasive alternative to tissue biopsy. Int J Mol Sci. 2018;19(10):2877.
14. Breitenbuecher F, Hoffarth S, Worm K, Cortes-Incio D, Gauler TC, Kohler J, et al. Development of a highly sensitive and specific method for detection of circulating tumor cells harboring somatic mutations in non-small-cell lung cancer patients. PLoS One. 2014;9(1):e85350.
15. Zhang Q, Nong J, Wang J, Yan Z, Yi L, Gao X, et al. Isolation of circulating tumor cells and detection of EGFR mutations in patients with non-small-cell lung cancer. Oncol Lett. 2019;17(4):3799–807.
16. Andergassen U, Kolbl AC, Mahner S, Jeschke U. Real-time RT-PCR systems for CTC detection from blood samples of breast cancer and gynaecological tumour patients (Review). Oncol Rep. 2016;35(4):1905–15.
17. Onidani K, Shoji H, Kakizaki T, Yoshimoto S, Okaya S, Miura N, et al. Monitoring of cancer patients via next-generation sequencing of patient-derived circulating tumor cells and tumor DNA. Cancer Sci. 2019;110(8):2590–9.
18. Liu Y, Liu B, Li XY, Li JJ, Qin HF, Tang CH, et al. A comparison of ARMS and direct sequencing for EGFR mutation analysis and tyrosine kinase inhibitors treatment prediction in body fluid samples of non-small-cell lung cancer patients. J Exp Clin Cancer Res. 2011;30:111.
19. Marchetti A, Martella C, Felicioni L, Barassi F, Salvatore S, Chella A, et al. EGFR mutations in non-small-cell lung cancer: analysis of a large series of cases and development of a rapid and sensitive method for diagnostic screening with potential implications on pharmacologic treatment. J Clin Oncol. 2005;23(4):857–65.
20. Asano H, Toyooka S, Tokumo M, Ichimura K, Aoe K, Ito S, et al. Detection of EGFR gene mutation in lung cancer by mutant-enriched polymerase chain reaction assay. Clin Cancer Res. 2006;12(1):43–8.
21. Piepenburg O, Williams CH, Stemple DL, Armes NA. DNA detection using recombination proteins. PLoS Biol. 2006;4(7):e204.
22. Li J, Macdonald J, von Stetten F. Review: a comprehensive summary of a decade development of the recombinase polymerase amplification. Analyst. 2018;144(1):31–67.
23. Daher RK, Stewart G, Boissinot M, Bergeron MG. Recombinase polymerase amplification for diagnostic applications. Clin Chem. 2016;62(7):947–58.
24. Wang R, Zhang F, Wang L, Qian W, Qian C, Wu J, et al. Instant, visual, and instrument-free method for on-site screening of GTS 40-3-2 soybean based on body-heat triggered recombinase polymerase amplification. Anal Chem. 2017;89(8):4413–8.
25. Crannell ZA, Rohrman B, Richards-Kortum R. Equipment-free incubation of recombinase polymerase amplification reactions using body heat. PLoS One. 2014;9(11):e112146.
26. Shi D, Huang J, Chuai Z, Chen D, Zhu X, Wang H, et al. Isothermal and rapid detection of pathogenic microorganisms using a nano-rolling circle amplification-surface plasmon resonance biosensor. Biosens Bioelectron. 2014;62:280–7.
27. Huang JF, Zhao N, Xu HQ, Xia H, Wei K, Fu WL, et al. Sensitive and specific detection of miRNA using an isothermal exponential amplification method using fluorescence-labeled LNA/DNA chimera primers. Anal Bioanal Chem. 2016;408(26):7437–46.
28. Qu XM, Ren XD, Su N, Sun XG, Deng SL, Lu WP, et al. Isothermal exponential amplification reactions triggered by circular templates (cEXPAR) targeting miRNA. Mol Biol Rep. 2023;50(4):3653–9.
29. Notomi T, Okayama H, Masubuchi H, Yonekawa T, Watanabe K, Amino N, et al. Loop-mediated isothermal amplification of DNA. Nucleic Acids Res. 2000;28(12):E63.
30. Nie Z, Zhao Y, Shu X, Li D, Ao Y, Li M, et al. Recombinase polymerase amplification with lateral flow strip for detecting Babesia microti infections. Parasitol Int. 2021;83:102351.
31. Choi G, Jung JH, Park BH, Oh SJ, Seo JH, Choi JS, et al. A centrifugal direct recombinase polymerase amplification (direct-RPA) microdevice for multiplex and real-time identification of food poisoning bacteria. Lab Chip. 2016;16(12):2309–16.
32. Srisrattakarn A, Panpru P, Tippayawat P, Chanawong A, Tavichakorntrakool R, Daduang J, et al. Rapid detection of methicillin-resistant Staphylococcus aureus in positive blood-cultures by recombinase polymerase amplification combined with lateral flow strip. PLoS One. 2022;17(6):e0270686.
33. Wang P, Ma C, Zhang X, Chen L, Yi L, Liu X, et al. A ligation/recombinase polymerase amplification assay for rapid detection of SARS-CoV-2. Front Cell Infect Microbiol. 2021;11:680728.
34. Shang M, Li J, Sun X, Su N, Li B, Jiang Y, et al. Duplex reverse transcription multienzyme isothermal rapid amplification assays for detecting SARS-CoV-2. Clin Lab. 2021;67(11):210239.
35. Jin CE, Yeom SS, Koo B, Lee TY, Lee JH, Shin Y, et al. Rapid and accurate detection of KRAS mutations in colorectal cancers using the isothermal-based optical sensor for companion diagnostics. Oncotarget. 2017;8(48):83860–71.
36. Liu Y, Lei T, Liu Z, Kuang Y, Lyu J, Wang Q. A novel technique to detect EGFR mutations in lung cancer. Int J Mol Sci. 2016;17(5):792.
37. Ren XD, Liu DY, Guo HQ, Wang L, Zhao N, Su N, et al. Sensitive detection of low-abundance in-frame deletions in EGFR

exon 19 using novel wild-type blockers in real-time PCR. Sci Rep. 2019;9(1):8276.
38. Su N, Wei K, Zhao N, Wang L, Duan GJ, Ren XD, et al. Sensitive and selective detections of codon 12 and 13 KRAS mutations in a single tube using modified wild-type blocker. Clin Chim Acta. 2019;494:123–31.
39. Choi MH, Kumara GSR, Lee J, Seo YJ. Point-of-care COVID-19 testing: colorimetric diagnosis using rapid and ultra-sensitive ramified rolling circle amplification. Anal Bioanal Chem. 2022;414(19):5907–15.
40. Li BW, Wei K, Liu QQ, Sun XG, Su N, Li WM, et al. Enhanced separation efficiency and purity of circulating tumor cells based on the combined effects of double sheath fluids and inertial focusing. Front Bioeng Biotechnol. 2021;9:750444.
41. Kalyan S, Torabi C, Khoo H, Sung HW, Choi SE, Wang W, et al. Inertial microfluidics enabling clinical research. Micromachines (Basel). 2021;12(3):257.
42. Di Carlo D. Inertial microfluidics. Lab Chip. 2009;9(21):3038–46.
43. Wu Z, Willing B, Bjerketorp J, Jansson JK, Hjort K. Soft inertial microfluidics for high throughput separation of bacteria from human blood cells. Lab Chip. 2009;9(9):1193–9.
44. Miyamoto DT, Sequist LV, Lee RJ. Circulating tumour cells-monitoring treatment response in prostate cancer. Nat Rev Clin Oncol. 2014;11(7):401–12.
45. Hwang WL, Hwang KL, Miyamoto DT. The promise of circulating tumor cells for precision cancer therapy. Biomark Med. 2016;10(12):1269–85.
46. Beije N, Jager A, Sleijfer S. Circulating tumor cell enumeration by the Cell Search system: the clinician's guide to breast cancer treatment? Cancer Treat Rev. 2015;41(2):144–50.
47. Yanagita M, Redig AJ, Paweletz CP, Dahlberg SE, O'Connell A, Feeney N, et al. A prospective evaluation of circulating tumor cells and cell-free DNA in EGFR-mutant non-small cell lung cancer patients treated with erlotinib on a phase II trial. Clin Cancer Res. 2016;22(24):6010–20.
48. Hwang WL, Pleskow HM, Miyamoto DT. Molecular analysis of circulating tumors cells: biomarkers beyond enumeration. Adv Drug Deliv Rev. 2018;125:122–31.
49. Tokumo M, Toyooka S, Ichihara S, Ohashi K, Tsukuda K, Ichimura K, et al. Double mutation and gene copy number of EGFR in gefitinib refractory non-small-cell lung cancer. Lung Cancer. 2006;53(1):117–21.
50. Cho H, Kim J, Song H, Sohn KY, Jeon M, Han KH. Microfluidic technologies for circulating tumor cell isolation. Analyst. 2018;143(13):2936–70.
51. Wu LL, Tang M, Zhang ZL, Qi CB, Hu J, Ma XY, et al. Chip-assisted single-cell biomarker profiling of heterogeneous circulating tumor cells using multifunctional nanospheres. Anal Chem. 2018;90(17):10518–26.
52. Nieto MA, Huang RY, Jackson RA, Thiery JP. Emt: 2016. Cell. 2016;166(1):21–45.
53. Micalizzi DS, Haber DA, Maheswaran S. Cancer metastasis through the prism of epithelial-to-mesenchymal transition in circulating tumor cells. Mol Oncol. 2017;11(7):770–80.
54. Naume B, Borgen E, Tossvik S, Pavlak N, Oates D, Nesland JM. Detection of isolated tumor cells in peripheral blood and in BM: evaluation of a new enrichment method. Cytotherapy. 2004;6(3):244–52.
55. Li M, Anand RK. High-throughput selective capture of single circulating tumor cells by dielectrophoresis at a wireless electrode array. J Am Chem Soc. 2017;139(26):8950–9.
56. Hoshino K, Huang YY, Lane N, Huebschman M, Uhr JW, Frenkel EP, et al. Microchip-based immunomagnetic detection of circulating tumor cells. Lab Chip. 2011;11(20):3449–57.
57. Wu M, Huang PH, Zhang R, Mao Z, Chen C, Kemeny G, et al. Circulating tumor cell phenotyping via high-throughput acoustic separation. Small. 2018;14(32):e1801131.
58. Descamps L, Le Roy D, Deman AL. Microfluidic-based technologies for CTC isolation: a review of 10 years of intense efforts towards liquid biopsy. Int J Mol Sci. 2022;23(4):1981.
59. Abdulla A, Zhang T, Ahmad KZ, Li S, Lou J, Ding X. Label-free separation of circulating tumor cells using a self-amplified inertial focusing (SAIF) microfluidic chip. Anal Chem. 2020;92(24):16170–9.
60. Wang Y, Gao W, Wu M, Zhang X, Liu W, Zhou Y, et al. EGFR mutation detection of lung circulating tumor cells using a multifunctional microfluidic chip. Talanta. 2021;225:122057.
61. Lee AC, Svedlund J, Darai E, Lee Y, Lee D, Lee HB, et al. OPENchip: an on-chip in situ molecular profiling platform for gene expression analysis and oncogenic mutation detection in single circulating tumour cells. Lab Chip. 2020;20(5):912–22.
62. Xu M, Zhao H, Chen J, Liu W, Li E, Wang Q, et al. An integrated microfluidic chip and its clinical application for circulating tumor cell isolation and single-cell analysis. Cytometry A. 2020;97(1):46–53.
63. Lobato IM, O'Sullivan CK. Recombinase polymerase amplification: basics, applications and recent advances. Trends Analyt Chem. 2018;98:19–35.